Pak. j. sci. ind. res. Ser. A: phys. sci. 2025 **68A**(3) ___-___

Efficient Removal of Heavy Metals from Water Using Magnetite Nanoparticles: Synthesis, Characterization and Adsorption Performance

Anwar A. Jumaa[a], Salwa A. Abduljaleel[b]*, Zuhair A. Abdulnabi[a] and Abdulzahra A.N. Alhello[a]
[a]Department of Marine Chemistry, Marine Science Center, University of Basrah, Basrah, Iraq
[b]Department of Biology, Faculty of Science, University of Basrah, Basrah, Iraq

(received March 26, 2024; revised November 6, 2024; accepted November 6, 2024)

Abstract. Nanomaterials, especially nanoparticles (NPs), have recently directed studies on mitigating water pollution due to their essential characteristics that make them very useful as sorbents. Here, a co-precipitation method is used to synthesize magnetite iron oxide (Fe_3O_4) NPs in order to employ them for remediating heavy metal-polluted effluents. The resulting Fe_3O_4 NPs are characterized by different techniques and tested for the removal of heavy metals from effluents of inner rivers in Basrah city, Iraq. FE-SEM analysis reveals spherical-like morphology of the NPs with an average size of 34.90 nm and zeta potential measurement indicates the presence of negative charge on their surface. Meanwhile, based on BET analysis, the surface area of the NPs is found to be 35.87 m^2/g. Adsorption experiments are utilized to select optimal conditions, taking into consideration of the influence of contact time, temperature and pH for heavy metal removal from simulated or polluted effluents. The results obtained demonstrate a high removal percentage (upto 94%) for Pb, Cd, Cu and Zn metals at room temperature for contact times ranging from 5 to 120 min and a concentration of 10 mg/L.

Keywords: magnetite nanoparticles, adsorption, water pollution, heavy metals

Introduction

Urbanization and industrialization make it more difficult for conventional water treatment methods to completely eliminate pollutants (Asghar *et al*., 2024). Given the current state of pollution, climate change and the recycling economy, pure water will become a valuable resource that requires sophisticated purification techniques like the usage of nanostructured adsorbents (Mudhoo and Sillanpaa, 2024). The primary source of physical, chemical (nutrients, metals, organic compounds and nanomaterials) and microbiological contamination of river water is agricultural runoff, which also includes municipal and industrial effluent. Industrial production, sewage, household garbage, municipal waste, retail establishments, dining establishments and agricultural waste are some of the sources of these wastes (Anawar *et al*., 2019).

The process of riverbank filtration is slow, natural and self-sustaining; it has no negative impacts. Chemical treatments are criticized for their high cost, possibility for secondary pollution and short-term remedy. Due to their high economic, environmental and ecological benefits, ease of maintenance and lack of secondary pollutants, ecological engineering-based techniques are preferred (Anawar and Chowdhury, 2020).

Thus, in water treatment applications, nanotechnology - a technology linked to the decrease of contaminants including bacteria, dangerous heavy metals, pesticides and other persistent and harmful chemicals has been utilized to address these issues. The main ways that humans are exposed to heavy metals and trace elements are through food and water, so determining the risk that these elements pose to humans through dietary and water consumption is crucial (Abduljaleel, 2016). In actuality, metals have been connected to a multitude of health issues, including encephalopathy, constipation, abdominal pain, lack of appetite, nausea, wakefulness, irritability and giddiness. Nonetheless, a number of studies have discovered a link between cancer and a patient's body's concentration of certain heavy metals such as Cd, Pb and Hg (Abduljaleel and Abdul Haleem, 2022). The world health organization (WHO) standard for the highest and maximum permissible limits, respectively of heavy metals in wastewater in mg/L such as Fe^{3+} (1.0 and 3.0), Cu^{2+} (0.5 and 2.0), Zn^{2+} (1.0 and 3.0), Pb^{2+} (0.01 and 0.4), Ni^{2+} (0.01 and 0.02), Cr^{6+} (0.05), Cd^{2+} (0.003 and 0.03), Mn^{2+} (0.4) (World health organization (WHO) standard, 1997). Nanostructured

*Author for correspondence;
E-mail: salwa.abduljaleel@uobasrah.edu.iq

materials are used for ecological recovery as they can potentially provide a cost-effective and efficient method for wastewater treatment (Dahiya *et al*., 2008). Magnetic nano adsorbents such as magnetite, maghemite and hematite are effective pollutant removers in wastewater. Due to their magnetic properties, they can be easily isolated from the reaction liquid by applying an external magnetic field. In addition, magnetite nanoparticles are known for their special properties, such as: B. their outstanding effectiveness in removing heavy metal ions such as lead, the avoidance of the creation of secondary waste, the creation of no secondary pollutants and the ability to treat large volumes of wastewater in a short time. Magnetite nanoparticles (NPs) with particle sizes smaller than 40 nm are easily dispersed in solutions, have a large surface area and are ferromagnetic due to the antiferromagnetically coupled Fe^{3+} cations in the tetrahedral and octahedral sites of their crystal structure, therefore magnetite is ferromagnetic with high magnetization (MS) and low coercivity (HC). They can be attracted to an externally induced magnetic field, but may lose their magnetic properties in the superparamagnetic state when the field is no longer present, depending on whether Fe_3O_4 is composed of single domain particles (Nguyen *et al*., 2021; Zhu *et al*., 2013; Abu Mukh-Qasem and Gedanken, 2005). Due to the magnetic properties of Fe_3O_4, they are effective agents for removing heavy metal ions and are extremely useful in innovative separation methods. In particular, Fe_3O_4 NPs have recently been proven to be excellent adsorbents for water purification due to their high area-to-volume ratio and fast magnetization reaction and adsorption processes (Agarwal and Singh, 2017; Türk and Alp, 2014). The goal of the current study is to extract heavy metals from contaminated water using magnetic Fe_3O_4 NPs.

Materials and Method

Description of the study area. Three samples were taken from the Al-khora, Al-ashar and Al-rebat canals, which are some of the inner channels of the Shatt al Arab river in the southern Iraqi city of Basra Governorate. Using a water sampler device and they were placed in a polyethylene container at a depth of 15 cm below the surface water in December 2022, during the winter. The location of these stations was determined using geological positioning system (GPS) as show in Table 1 and Fig. 1.

After collecting, the samples were immediately measured the some chemophysical properties in the field using a multimeter (Multi 3210) from WTW, Germany (Table 2) and then they preserved by adding 1 mL of nitric acid and kept in a cool place. The samples were transported to the laboratory for carrying out the filtration process in order to remove any suspended materials.

The $FeCl_3.6H_2O$ and $FeSO_4.7H_2O$ were supplied by Sigma-Aldrich and the ammonia solution (25% v/v), 1000 mg/L of standards solution for Zn, Pd, Cu and Cd

Table 1. The locations of sub-channels selected stations

Station	Al-khora	Al-ashar	Al-rebat
Location	E 475101 N 30°30'32".93	E 475018.2 N 30°31'19".58	E 4749 57.49 N 30°31'48".97

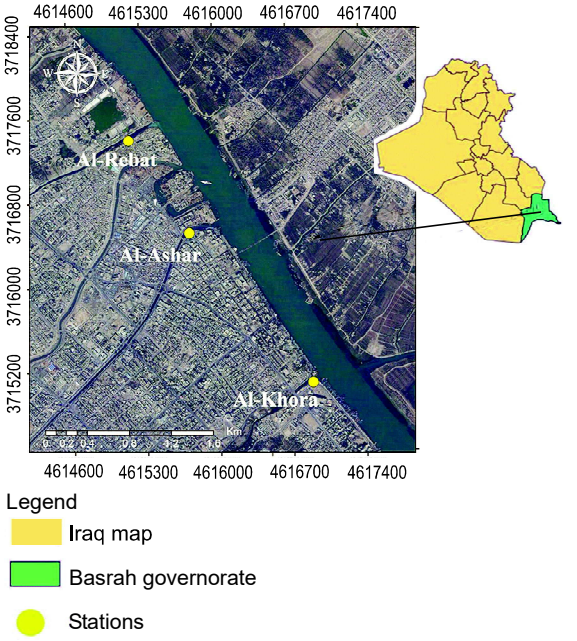

Fig. 1. A map of Shatt Al-arab and the sampling stations.

Table 2. The chemo-physical properties of selected samples

Station	pH	Temperature °C	TDS ppm	Salinity ppt
Al-khora	7.83	17.1	3942.4	3.8
Al-ashar	7.81	18.1	4739.6	4.6
Al-rebat	8.13	17.9	2867.2	2.6

and sodium hydroxide were supplied from Merck. Hydrochloric acid and nitric acid were obtained by G.C.C.

Instrumentation. The chemophysical properties were measured using a multimeter (Multi 3210) from WTW, Germany. The shaking incubator was used for agitating samples model Certomat IS, Germany. All measurements of the heavy metal ions were obtained by a wavelength at 226.5, 324.7, 220.3 and 213.8 nm for cadmium, copper, lead and zinc ions respectively using the inductive coupled plasma instrument type ICP-OES, Thermo Fisher Scientific, Germany.

Characterization of nanoparticles. Fe_3O_4 nanoparticles were characterized by nanotechnology using BET, VSM, Zeta potential, X-ray diffraction studies (XRD), SEM, and EDX.

Synthesis of Fe_3O_4 MNPs. The co-precipitation method used to create Fe_3O_4 MNPs was as follows: Deionized water (100 mL) in a beaker. The pH of the solution reached 12 after 2 to 1 mole of $FeCl_3.6H_2O$ and $FeSO_4.7H_2O$ powder were dissolved in deionized water under magnetic stirring for 10 min at room temperature. 0.25 mL of NH_4OH, diluted in 75 mL of deionized water, was then added dropwise to the above solution and left for approximately 1 h under magnetic stirring at room temperature. The black powder precipitate was separated with external magnet, centrifuged and washed several time using deionized water and ethanol to remove unreacted ions. Finally, the precipitate was dried for 6 h in an oven at 90 °C (Khalaji *et al*., 2021). Figure 2 show co-precipitation methods used for synthesis of Fe_3O_4 MNPs.

Preparation the polluted water. In order to study the treatment of polluted water by some heavy metals, therefore the collected samples were contaminated by 10 mg/L standard solutions to each of the elements such as zinc, lead, copper and cadmium. Three polluted samples of heavy metal ions were prepared by taking 10 mL of each of the standard solutions (1000 mg/L) for heavy metals and transporting them to a volumetric 1000 mL and then they were diluted by a polluted water sample.

Treatment study of the polluted water. After polluting the collected sample for three stations. The treatment process was carried out using the adsorption experiments in order to achieve the optimal conditions for removing of these elements together such as contact time, temperature and pH level onto the prepared adsorbent

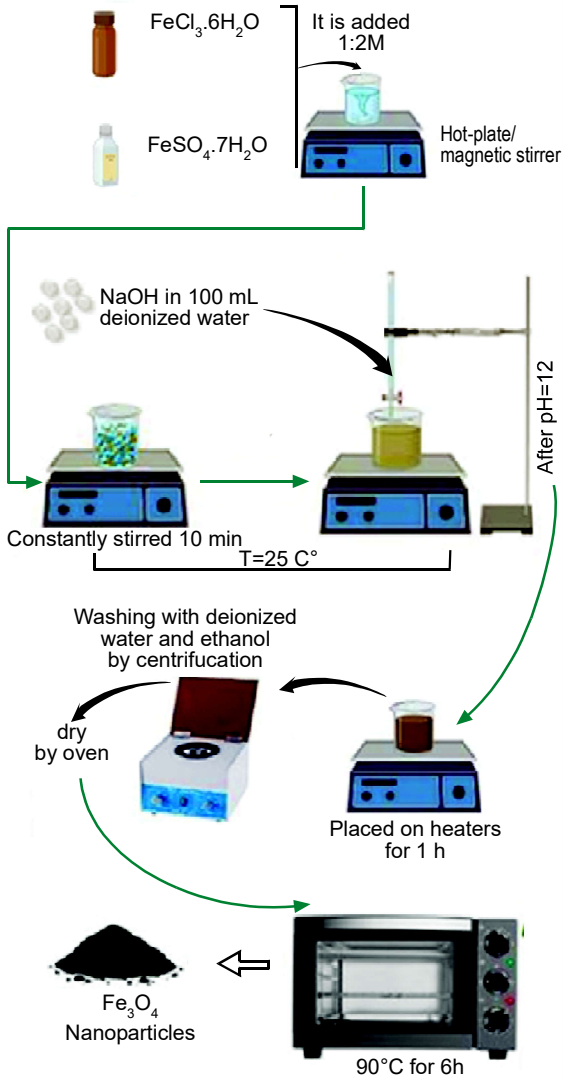

Fig. 2. The steps co-precipitation of synthesis of Fe_3O_4 MNPs.

surface by fixing the other parameters such as initial concentration 10 mg/L of each the metals, weight amount 0.05 g, mixing speed 120 rpm, temperature at 25 °C and volume of heavy metals solution 10 mL.

Recovery study. After the completed adsorption process for heavy metal ions onto magnetite surface. The recovery experiment was carried out using 0.5 N of HCl, in order to give a good, understand about the bonded and rejected mechanisms among heavy metal ions with the magnetite surface.

Results and Discussions

Characterization of the magnetite (Fe_3O_4). ***Analysis of scanning electron microscopy (SEM).*** New physical

properties are revealed as the particle size of solid materials is reduced to the nanoscale realm. The material properties varies substantially from those at larger scales due to the varied shapes of nanoparticles. Materials' shape, size and morphology can greatly alter how they interact with heavy meal contaminants, for instant and so their size and surface roughness ultimately affect the practicality and quality of materials. The well-known quantum confinement phenomenon, which appears at the nanoscale, governs the adsorption properties of magnetic nanoparticles. As a result, the size and geometry of the nanoparticles influence the adsorption properties significantly. SEM micrographs of the sample surfaces were obtained in order to analyze the morphology and describe the surface of the Fe_3O_4 particles. The consequences of grain size and shape on the adsorption characteristics of the generated materials were assessed using SEM micrograph. Fig. 3 displays particle size histograms for each image of the Fe_3O_4 nanoparticles recorded using scanning electron microscopy (SEM). The Image-J is used image analysis tool to obtain a statistical interpretation of the data. This tool is used to create the size distribution of each histogram that is associated to each image by estimating the number of particle diameters from micrograph. The histograms (constant red line) for each size distribution were fitted with a Gaussian function, from which the median, mean value of the distribution and standard deviation could be calculated in Table 3. The results revealed that the synthetic Fe_3O_4 nanoparticles are almost non-regular cubic-like in shape and nearly mono-disperse. Due to the high surface energy of Fe_3O_4 nanoparticles, there are only a small number of larger aggregates in the sample.

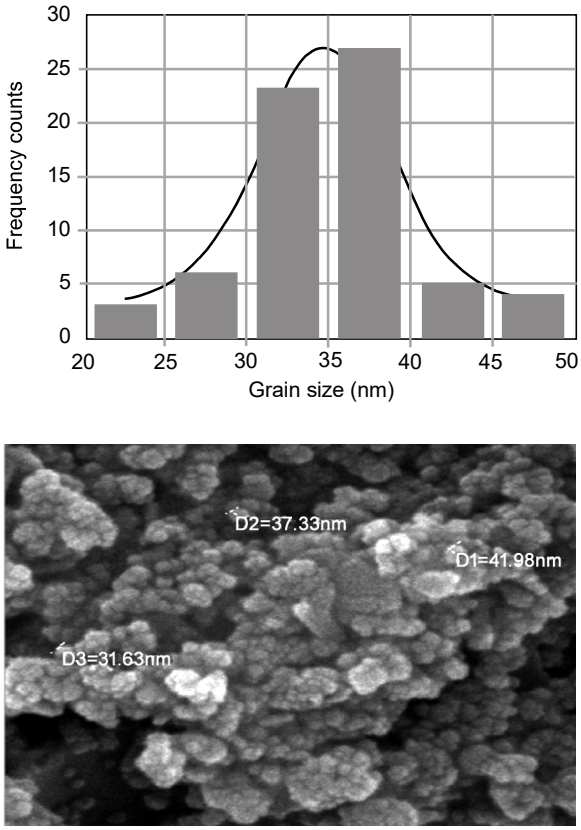

Fig. 3. Analysis of scanning electron microscopy (SEM).

Table 3. The results of grain size analysis

Sample	Mean (nm)	Standard deviation	Minimum (nm)	Median (nm)	Maximum (nm)
Fe_3O_4	34.900	4.888	23.3	35	47.2

Selected of the magnetic properties. The vibrated sample magnetometer (VSM) [MDK Iran] device with a very precise measurement protocol was used to characterize the magnetic properties of the synthesized magnetite powder. To describe magnetism in materials, three parameters were calculated: remanence magnetization (Mr), coercivity force (Hc) and saturation magnetization (Ms). The (Mr) value quantifies a material's magnetic strength in the absence of an external magnetic field. The coercive field, also recognized as the value (Hc), determines whether a magnetic substance can continue to be magnetized in an external field. (BH)max denotes the maximum product of an induced magnetization value and the corresponding applied field. Many magnetic materials still have high (Mr) or high (Hc) values but these attributes do not always translate into high (BH)max quantities. Magnetic properties were measured for two samples at 300 K with a static maximum field of 5000 Oe (Li *et al*., 2015; Coey, 2012), as shown in Fig. 4. Table 4 depicts the coercive field, saturation magnetization and remnant magnetization. The switching field distribution (SFD: dM/dH) is a significant and essential micromagnetic characteristic curve representation that depicts the reversal state of particle distribution in the right panel of Fig. 5.

X-ray diffraction analysis. Using special techniques, various information about materials can be obtained, such as information about crystal size, the arrangement

of atoms in the crystal lattice and the crystalline phase. Therefore, XRD spectroscopy was used to obtain this information but on the other hand it was also used to characterize the different materials (Abdulnabi *et al*., 2021). The extracted data of the XRD pattern showed a variability band at the 2θ position (30.0°, 33.42°, 36.89°, 43.38°, 44.58°, 57.30° and 62.91°) and had FWHM values (0.3936, 0.1968, 0.3936, 0.2952, 0.3936, 0.4920 and 0.5904 2θ, respectively). This results are corresponding with previous studies (Chaki *et al*., 2015; Loh *et al*., 2008). The average crystal size was calculated using the Debye-Sherrer equation and gave a value of 17.837 nm. The X-ray diffraction pattern is shown in Fig. 6.

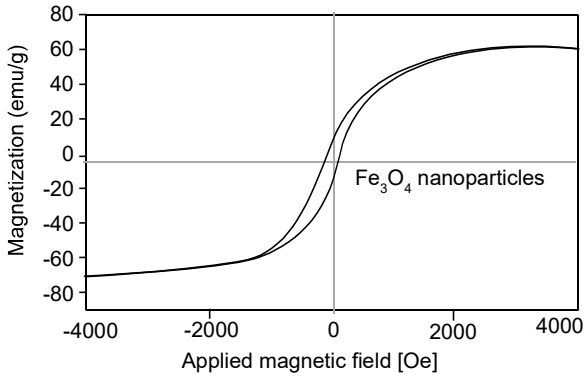

Fig. 4. The analysis of magnetic properties of Fe_3O_4.

Table 4. The results of magnetic analysis of Fe_3O_4

Sample	Saturation magnetization (MS)(emu/g)	Remanence magnetization (Mr) (emu/g)	Coercive field (Hc)(Oe)
Fe_3O_4	52.326	6.489	71

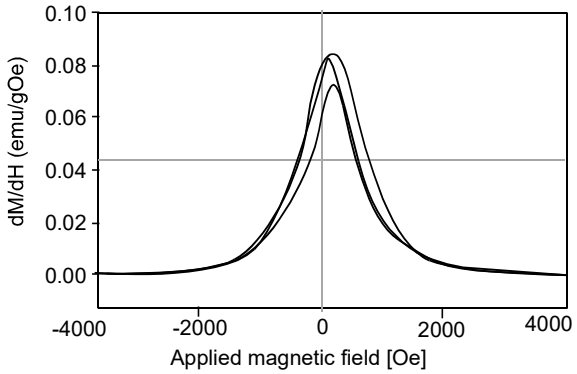

Fig. 5. The essential micromagnetic characteristic curve of Fe_3O_4.

Determination of zeta potential. Some essential requirements for adsorption experiments are the stability of solid materials in aqueous solutions and their surface charge. After manufacturing, nanoparticles undergo the agglomeration process over time, which results in a reduction in the surface area of the solid material as the particle size increases (Abdulnabi *et al*., 2022). Therefore, the stability and surface charge of the prepared compound were selected by measuring the zeta potential. Iron oxide (Fe_3O_4) in its aqueous solution exhibits stability, a negative surface charge and an average zeta potential value of -31.6 mV. A negative value of the adsorbent surface that helps to increase attraction with positive ions and then obtain a high removal efficiency for heavy metal ions. The zeta potential results are shown in Fig. 7.

Surface area and porosity analyses. Basically, the adsorption efficiency of an adsorbent surface depends

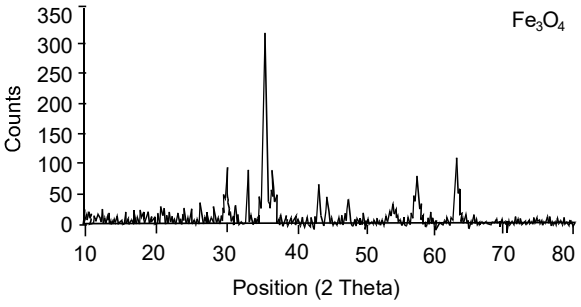

Fig. 6. The XRD pattern of Fe_3O_4.

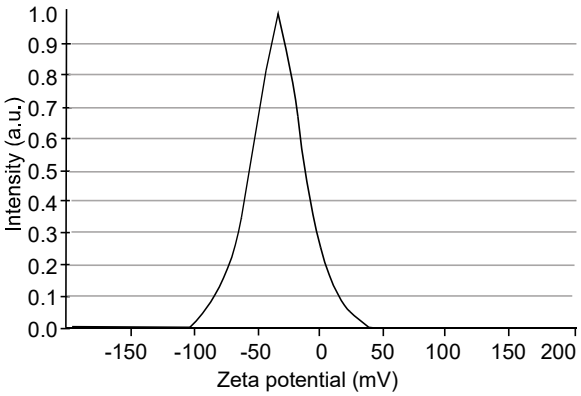

Fig. 7. Zeta potential of Fe_3O_4.

on the functional groups and pore structures on its outer surface (Mizhir *et al*., 2020). On the other hand, the structural pore can be divided into three types: micropores, mesopores and macropores (Abdulnabi, 2021). There are many methods for selecting the surface of materials such as Langmuir, Brunauer Emmett Teller (BET), Barrett Joyner Halenda (BJH) and T-Plot using inert gases such as nitrogen and a temperature of 77 K at which the molecules of the inert gas are formed use the occupation of all active sites on the outer surface of materials and thus the number of these desorption molecules indicates the surface value (Abdulnabi, 2021). The BET and BJH methods were used to calculate the magnetite surface area and pore structure type. The results revealed a surface area of 35.89 m^2/g and a mesopore structure.

Energy dispersive X-ray analysis (EDX). EDX analysis has been used to characterize the elemental composition of materials. This technique was applied at room temperature and voltage acceleration in the range of 0-80 KeV (Radhi, 2019). The data explained in Table 5 and Fig. 8 appeared to contain iron and oxygen, confirming the formation of magnetite.

Physico-chemical properties of waste water. Three locations were selected from some sub-channels of the Shatt Al-arab river such as Al-khora, Al-ashar and Al-rebat. The results are presented in Table 2 and showed acid function (pH) values ranging from 7.81 to 8.13, which were within the locally and globally acceptable limit. The total dissolved solids (TDS) was recorded in the range of 2867.2 to 4739.6 ppm classified as slightly brackish water according to the classification scheme of Carrol (Pradhan and Piraste, 2011). While the salinity should have values in the range of 2.6-4.6 g/L, this value refers to the salinity and ionic strength of the water samples collected.

Heavy metals measurement in wastewater. ***Lead ion (Pb^{2+}).*** The results in the Table 6 showed clear contamination with lead in both the study station within the Al-khora and Al-ashar channels, while the result of the measurement was N.D in the Rebat channel. This is due to surface runoff or carrying lead formed as a result of industrial processes and internal combustion engines, thus washing into the channel water with rain and surface flow (Al-Asadi *et al*., 2019).

Cadmium ion (Cd^{2+}). Because there were comparatively few human activities that produced cadmium in the Al-rebat river and Al-khora channels, the results indicated that the cadmium concentration, as shown in Table 6, was within the World Health Organization's allowable limits and the standard parameters for Iraqi waters. Due to human activities that are concentrated in the Al-ashar channel there is a higher flow of sewage or emissions from internal combustion engines that reach the river water through surface flow of rainwater. As a result, the concentration of cadmium in the Al-ashar channel was higher than allowable limits (Hassan *et al*., 2017)

Zinc and Copper ions (Zn^{2+}, Cu^{2+}). The results shown in the Table 6 a decrease in Cu and Zn ions concentrations in all channels included in the study, except for the Cu values within the Rebat which was undetectable (N.D). The low concentrations of these metals in channel water is due to their low solubility in water, in addition to the fact that they are heavy elements that are associated with suspended colloids through the

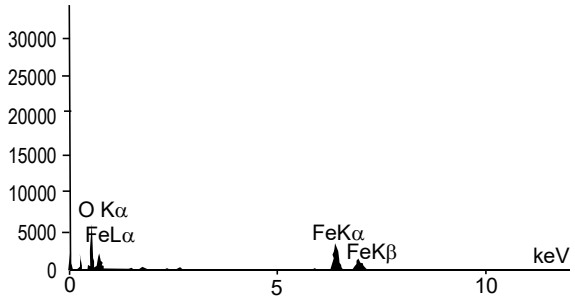

Fig. 8. EDX analysis of Fe_3O_4.

Table 5. The elemental composition

Material	Elemental percent		Total percent
	Fe	O	
Fe_3O_4	57.18	42.82	100

Table 6. Lead, cadmium, cooper and zinc concen-tration in selected sample

Heavy metal	Unit	Standard specifications		Concentration of heavy metals in study area samples		
		IQR (2009)	WHO (2018)	Al-khora	Al-ashar	Al-rebat
Pb	mg/L	0.01	0.01	0.1825	0.0391	N.D
Cd	mg/L	0.003	0.003	0.002	0.0051	0.001
Cu	mg/L	1	2	0.0069	0.0025	N.D
Zn	mg/L	3	3	0.029	0.0216	0.0246

adsorption process (Mimba *et al*., 2017). This may be due to the alkaline environment of the region, where the pH values in the water of the study area were recorded within the basic limits of the water, where the highest pH values reached 8.13 and this enhances its insolubleness. Low concentrations may be indicators of the limited impact of human activities on these elements. This observation can be attributed to the fact that most factories stopped working during the study period. The effect of wastewater discharge on heavy elements levels in river water may be limited, because heavy elements concentrations in domestic wastewater were low. Al-ashar, Al-rebat and Al-khora channels were also closed for cleaning during the study period. In addition, seawater chemistry in the Arabian Gulf contains lower levels of heavy elements, ranging between 0 and 0.78 µg/L (Al-Asadi *et al*., 2019; Manavi, 2013). Therefore, the tide reduces the levels of heavy element in the river through mixing and dilution processes as a result of the change in the flow direction of the Gulf water during the tides.

Removal of heavy metals on magnetite surfaces. Three simulated contaminated wastewater samples were prepared using standard solutions of lead, zinc, copper and cadmium and then many processes were carried out to remove these elements through adsorption on the magnetite surface, such as contact time, temperature and pH tests. Removal percent was given by the relationship (Abdulnabi *et al*., 2022; Radhi, 2019).

$$\%R=(C_o-C_e/C_o)\times 100$$

where:
C_o is initial concentration of metals ions, C_e is concentration of metals ions at equilibrium state

Effect of contact time. The influence of contact time was studied on the effectiveness of removal of four heavy metals at room temperature for periods ranging from 5 to 120 min and the other parameters such as concentration (10 mg/L), amount of adsorbent (0.05 g) and stirring speed were established (120 rpm), 10 mL heavy metal solutions and natural pH value of the solutions. The data showed a high removal percentage for lead, zinc, copper and cadmium. A minimum contact time was found for zinc than other elements that can form a strong bond with the magnetite surface, while a maximum contact time was found for cadmium (Fig. 9), which is due to the increase in its radius (Lin *et al*., 2019). In general, converging values were recorded for removal percentage for elements. All results are shown in Table 7.

Effect of temperature. The temperature factor is an important parameter for selecting the type of adsorption material in view of the type of bonding between adsorbent and adsorbate (Abdulnabi, 2021). The percentage of removal of all heavy metal ions was applied at different temperatures ranging from 20 °C to 50 °C and the remaining parameters were determined. The results showed the highest removal percentage in

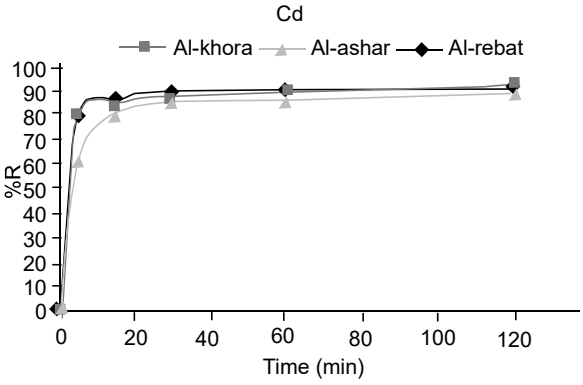

Fig. 9. Effect of contact time selected of cadmium.

Table 7. Removal percent at equilibrium time

Station	Lead		Zinc		Copper		Cadmium	
	%R ($C_e$ppm)	Contact time (min)	%R ($C_e$ppm)	Contact time (min)	%R ($C_e$ppm)	Contact time (min)	%R ($C_e$ppm)	Contact time (min)
Al-khora	90.9002 (0.910)	15	90.8639 (0.913)	5	91.2492 (0.875)	15	90.0125 (0.998)	60
Al-ashar	90.9637 (0.903)	15	90.8853 (0.911)	5	91.8813 (0.811)	15	84.9171 (1.508)	30
Al-rebat	90.9650 (0.903)	5	90.8398 (0.916)	5	92.2123 (0.778)	30	89.5226 (1.047)	30

all polluted stations on the magnetite surface, as the bonding strength between the adsorption surface with metal ions, especially zinc ions increased, on the other hand, the removal percentage increased as the temperature point decreased to form a weak bond due to different charges (Sepulveda and Santana, 2013), this result corresponds to the zeta potential data. All results are shown in Table 8 and Figs. 10 and 11.

Effect of acidic function. After selecting the best conditions such as contact time and temperature, the pH was determined under three values of acid function at 3, 6 and 9, while the other parameters such as adsorbent weight (0.05 g), volume of heavy metal solution (10 mL), stirring speed (120 rpm), contact time (60 min.) and temperature (20 °C). The results are presented in Table 9 and showed the highest removal efficiency for lead, copper and zinc at all pH values examined, while increasing removal of cadmium ions (Fig. 12) occurred gradually with an increase in pH values towards the basic medium, which is possibly due to a charge exchange between the magnetite surface and heavy metal ion solution (Sepulveda and Santana, 2013). Furthermore, most of the metal ions precipitated with an increase in pH toward the basic medium (Prokkola *et al*., 2020; Mlayah and Jellali, 2015).

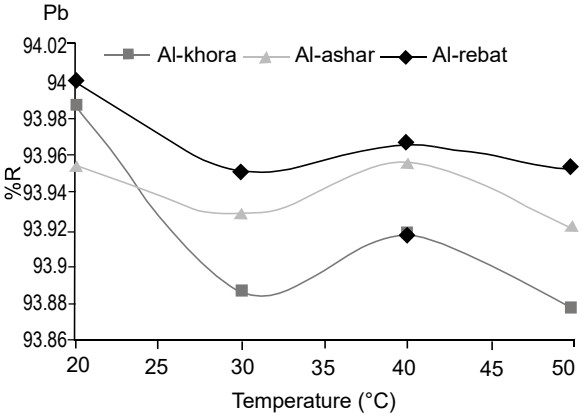

Fig. 11. Temperature effect on removal efficiency for lead ions.

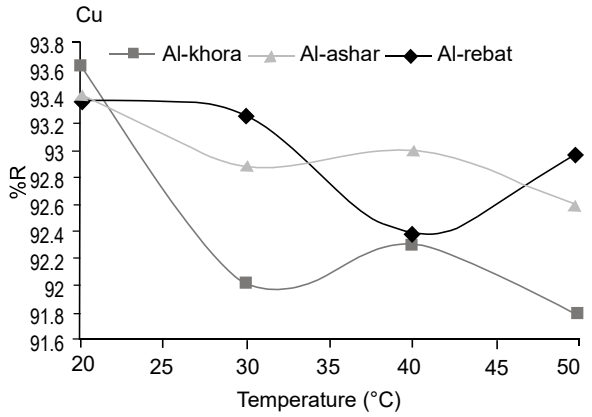

Fig. 10. Temperature effect on removal efficiency for copper ions.

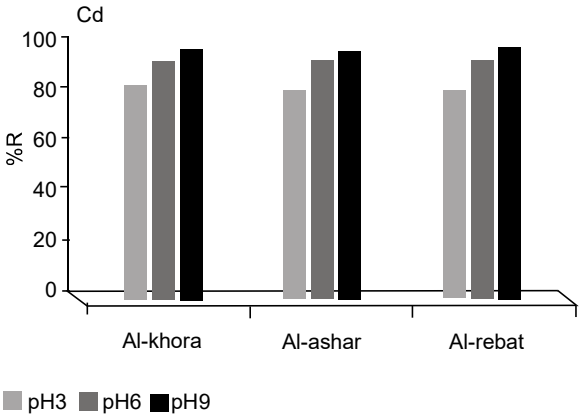

Fig. 12. pH selected of cadimum onto magntite surface.

Table 8. Effect temperature on removal efficiency

Station	Lead		Zinc		Copper		Cadmium	
	%R ($C_e$ppm)	Temperature (°C)	%R ($C_e$ppm)	Temperature (°C)	%R ($C_e$ppm)	Temperature (°C)	%R ($C_e$ppm)	Temperature (°C)
Al-khora	93.9863 (0.601)	20	94.00 (0.600)	20	93.6244 (0.637)	20	90.8714 (0.912)	20
Al-ashar	93.9538 (0.604)	20	94.00 (0.600)	20	93.4298 (0.657)	20	91.0835 (0.891)	30
Al-rebat	94.00 (0.600)	20	94.00 (0.600)	20	93.3728 (0.662)	20	90.7849 (0.921)	30

Table 9. Effect of pH on removal efficiency

Station	Lead		Zinc		Copper		Cadmium	
	%R ($C_e$ppm)	pH	%R ($C_e$ppm)	pH	%R ($C_e$ppm)	pH	%R ($C_e$ppm)	pH
Al-khora	100 (0.00)	6	100 (0.00)	6	100 (0.00)	6	97.1939 (0.280)	9
Al-ashar	100 (0.00)	6	100 (0.00)	6	100 (0.00)	6	95.6684 (0.433)	9
Al-rebat	100 (0.00)	6	100 (0.00)	6	100 (0.00)	6	97.5150 (0.248)	9

Therefore, the best pH value of 6 was chosen in the current study. The selected conditions appeared to have the highest removal percentage for all heavy metals on the magnetite surface, possibly due to an increase in surface area with reduced particle size, which is consistent with the BET, XRD and SEM analyses.

Recovery experiment. Using 0.5 M of hydrochloric acid solution for three hours at room temperature, the recovery efficiency of magnetite to recapture heavy metals after they have been removed on the magnetite surface under ideal conditions, including contact time, temperature, pH level, agitation pH, stirring speed, adsorbent weight and volume of heavy metals ions solution. While cadmium ions were more frequently collected than other metal ions in Al-ashar and Al-rebat stations, the results showed that lead had the highest recovery percentage among other metals in the Al-khora station as in Table 10 and Fig. 13. The low recovery level could be the result of a drop in the acidic concentration because the recovery process generally depends on utilizing an acidic solution to break the bindings between the magnetite surface and metal ions

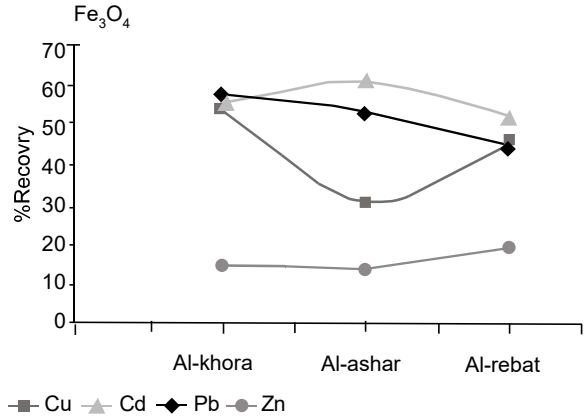

Fig. 13. Recovery percent of heavy metals ions.

Table 10. Recovery percent of magnetite surface

Station	Lead %recovery	Zinc %recovery	Copper %recovery	Cadmium %recovery
Al-khora	57.792	14.645	53.937	55.454
Al-ashar	53.194	14.111	30.343	60.893
Al-rebat	44.174	18.716	45.624	51.688

(Momina *et al*., 2019). Consequently, a decrease in the solution's acidic concentration and an increase in their strong connection could be the cause of the low recovery level.

Conclusions

Using magnetite nanoparticles, the data demonstrated high removal percentages for lead, zinc, copper and cadmium at room temperature for durations ranging from 5 to 120 mins. Other parameters, including concentration (10 mg/L), also showed high removal percentages for Zn, Pb, Cu and Cd. The magnetite nanoparticles were prepared by a chemical process and achieved a high yield. To detect the formation of nanoparticles, several identification techniques have been used. The prepared nanoparticles have stability, negative charge, magnetic properties and a large surface area. These properties result in the highest percentage of lead, zinc, copper and cadmium being removed from simulated wastewater. The recovery ratio of cadmium ions was significantly increased compared to other heavy metal ions. The FeO4 NPs be further modified to enhance their performance to remove toxic metals from wastewater.

Acknowledgement

The author thanks Dr. Hashim Jabber, Department of Physics, College of Science, University of Basrah for his kind assistance in measuring and analyzing of the data of vibrating sample magnetometer and for his qualitative cooperation in interpretation of the magnetic effect of nanoparticles.

Conflict of Interest. The authors declare that they have no conflict of interest.

References

Abduljaleel, S.A. 2016. Determination of some trace elements in chicken eggs from different sources. *Journal of Pharmacognosy and Phytochemistry*, **5:** 417-420.

Abduljaleel, S.A., Abdul Haleem, E. 2022. Relationship between trace elements levels and lung cancer patients in southern Iraq. *Asian Journal of Research Zoology*, **5:** 54-64.

Abdulnabi, Z.A. 2021. Synthesis and Characterization of Some Selenazone Complexes and Nanoadsorbent Surfaces from Industrial Waste for Removing Some Carcinogenic Dyes and Heavy Metals from Water. *Ph.D. Thesis*, 293 pp., University of Basra, Iraq.

Abdulnabi, Z.A., Abdulsahib, H.T., Al-doghachi, F.A.J. 2022. Extraction of nanomaterial from soot waste as low-cost adsorbent for removal of some carcinogenic dyes from aqueous solution. *Indian Journal of Ecology*, **49:** 610-617.

Abdulnabi, Z.A., Al-doghachi, F.A.J., Abdulsahib, H.T. 2021. Synthesis, characterization and thermo-gravimetric study of some metal complexes of selenazone ligand nanoparticles analogue of dithizone. *Indonesian Journal of Chemistry*, **21:** 1231-1243.

Abu Mukh-Qasem, R., Gedanken, A. 2005. Sono-chemical synthesis of stable hydrosol of Fe_3O_4 nanoparticles. *Journal of College International Science*, **284:** 489-494.

Agarwal, R.M., Singh, K. 2017. Heavy metal removal from wastewater using various adsorbents: a review. *Journal of Water Reuse and Desalination*, **4:** 387-419.

Al-Asadi, S.A.R., Al Hawash, A.B., Alkhlifa, N.H., Ghalib, H.B. 2019. Factors affecting the levels of toxic metals in the Shatt Al-Arab river, southern Iraq. *Earth System and Environment*, **3:** 313-325. DOI: 10.1007/s41748-019-00096-y

Anawar, H.M., Strezov, V. 2019. Transport, fate and toxicity of the emerging and nanomaterial contaminants in aquatic ecosystems: removal by natural processes. In: *Emerging and Nanomaterial Contaminants in Wastewater. Advanced Treatment Technologies*, Mishra, A.K., Anawar, H.M., Nadjib, D., (eds.), 1st edition, Elsevier Cambridge, CA, USA.

Anawar, M.H., Chowdhury, R. 2020. Remediation of polluted river water by biological, chemical, ecological and engineering processes. *Sustainability*, **12:** 7017.

Asghar, N., Alamdar, H., Duc Anh, N., Salar, A., Ishtiaque, H., Aurangzeb, J., Attarad, A. 2024. Advancement in nanomaterials for environmental pollutants remediation: a systematic review on bibliometrics analysis, material types, synthesis pathways and related mechanisms. *Journal of Nanobiotechnology*, **22:** 26. https://doi.org/10.1186/s12951-023-02151-3

Chaki, S.H., Malek, T.J., Chaudhary, M.D., Tailor, J.P., Deshpande, M.P. 2015. Magnetite Fe_3O_4 nano-particles synthesis by wet chemical reduction and their characterization. *Advances in Natural Sciences, Nanoscience and Nanotechnology*, **2015:** 6. Doi: 10.1088/2043-6262/6/3/035009.

Coey, J.M.D. 2012. *Magnetism and Magnetic Materials*, Cambridge University Press, 2012. Doi:1017/CBO9780511845000

Dahiya, S., Tripathi, R.M., Hegde, A.G. 2008. Biosorption of heavy metals and radionuclide from aqueous solutions by pre-treated arca shell biomass. *Journal of Hazardous Materials*, **150:** 376-386.

Hassan, W.F., Hassan, I.F., Al-Khuzaie, D.K.K., Abdulnabi, Z.A., Khalaf, H.H., Kzaal, R.S., Almansour, W.A. 2017. Monitoring of trace elements in dust fallout in Shaibah, Basrah city, Iraq. *Mesopotamia Environmental Journal*, **4:** 35-41.

Khalaji, A.D., Machek, P., Jarosova, M. 2021. α-Fe_2O_3 nanoparticles: synthesis, characterization, magnetic properties and photocatalytic degradation of methyl orange. *Advanced Journal of Chemistry-Section A*, **4:** 317-326. DOI: 10.22034/ajca.2021.292396.1268

Li, Y., Xu, B., Hu, S., Li, Yu., Li, Q., Liu, W. 2015. Simulation of magnetic hysteresis loops and magnetic Barkhausen noise of α-iron containing nonmagnetic particles. *AIP Advances*, **5:** 1-7.

Lin, D.J., Wang, L., Wang, X.D., Yan, W.M. 2019. Reduction in the contact time of impacting droplets by decorating a rectangular ridge on superhydrophobic surfaces. *International Journal of Heat and Mass Transfer*, **132:** 1105-1115.

Loh, K.S., Lee, Y.H., Musa, A., Salmah, A.A., Zamri, I. 2008. Use of Fe_3O_4 nanoparticles for enhancement of biosensor response to the herbicide 2,4-Dichlorophenoxyacetic acid. *Sensors*, **8:** 5775-5791.

Manavi, P.N. 2013. Heavy metals in water, sediment and macrobenthos in the interdidal zone of Hormozgan province. *Iranian Marin Science*, **3:** 39-47. DOI:10.5923/j.ms.20130302.0

Mimba, M.E., Ohba, T., Nguemhe Fils, S.C., Wirmvem, M.J., Numanami, N., Aka, F.T. 2017. Seasonal hydrological inputs of major ions and trace metal composition in streams draining the mineralized Lom basin, east Cameroon: basis for environmental

studies. *Earth Systems and Environment*, **1:** 1-9. DOI: 10.1007/s41748-017-0026-6

Mizhir, A.A., Abdulwahid, A.A., Al-Lami, H.S. 2020. Adsorption of carcinogenic dye Congo red onto prepared graphene oxide-based composites. *Desalination and Water Treatment*, **202:** 381-395.

Mlayah, A., Jellali, S. 2015. Study of continuous lead removal from aqueous solutions by marble wastes: efficiencies and mechanisms. *International Journal of Environmental Science and Technology*, **12:** 2965-2978.

Momina, R.M., Ismail, S., Ahmad, A. 2019. Study for the desorption of methylene blue dye from clay based adsorbent coating. *Water*, **11:** 1304.

Mudhoo, A., Sillanpaa, M. 2021. Magnetic nano-adsorbents for micropollutant removal in real water treatment: a review. *Environmental Chemistry Letters*, **19:** DOI: 10.1007/s10311-021-01289-6.

Nguyen, M.D., Tran, H.V., Xu, S., Lee, T.R. 2021. Fe_3O_4 nanoparticles: structures, synthesis, magnetic properties, surface functionalization and emerging applications. *Applied Science*, **11:** 11301. Doi: 10. 3390/app112311301.

Pradhan, B., Piraste, S. 2011. Hydro-chemical analysis of the ground water of the basaltic catchments: upper Bhatsai region, Maharastra. *The Open Hydrology Journal*, **5:** 51-57.

Prokkola, H., Nurmesniemi, E.T., Lassi, U. 2020. Removal of metals by sulphide precipitation using Na_2S and HS-solution. *Chemical Engineering*, **4:** 51.

Radhi, I.K. 2019. Removing Some Anionic Dyes by Modification of CaO Derived from Eggshell and Study of Adsorption, Kinetic, Thermodynamics and Photocatalytic Characteristics. *Ph.D Thesis*, 230 pp., University of Basra, Iraq.

Sepulveda, L.A., Santana, C.C. 2013. Effect of solution temperature, pH and ionic strength on dye adsorption onto Magellanic peat. *Environmental Technology*, **34:** 967-977.

Türk, T., Alp, I. 2014. Arsenic removal from aqueous solutions with Fe-hydrotalcite supported magnetite nanoparticle. *Industrial and Engineering Chemistry*, **20:** 732-738.

WHO, *1997*. *Food Consumption and Exposure Assessment of Chemicals*. Report of an FAO/WHO Consultation on Food Consumption and Exposure Assessment of Chemicals, Geneva, World Health Organization.

Zhu, J., Wei, S., Chen, M., Gu, H., Rapole, S.B., Pallavkar, S., Ho, T.C., Hopper, J., Guo, Z. 2013. Magnetic nanocomposites for environmental remediation. *Advance Powder Technology*, **24:** 459-467.